A novel 4H-SiC lateral bipolar junction transistor structure with high voltage and high current gain*

Deng Yong-Hui(邓永辉), Xie Gang(谢 刚)†, Wang Tao(汪 涛), and Sheng Kuang(盛 况)

College of Electrical Engineering, Zhejiang University, Hangzhou 310007, *China*

(Received 17 December 2012; revised manuscript received 12 March 2013)

In this paper, a novel structure of a 4H-SiC lateral bipolar junction transistor (LBJT) with a base field plate and double RESURF in the drift region is presented. Collector-base junction depletion extension in the base region is restricted by the base field plate. Thin base as well as low base doping of the LBJT therefore can be achieved under the condition of avalanche breakdown. Simulation results show that thin base of 0.32 μm and base doping of 3×10^{17} cm^{-3} are obtained, and corresponding current gain is as high as 247 with avalanche breakdown voltage of 3309 V when the drift region length is 30 μm. Besides, an investigation of a 4H-SiC vertical BJT (VBJT) with comparable breakdown voltage (3357 V) shows that the minimum base width of 0.25 μm and base doping as high as 8×10^{17} cm^{-3} contribute to a maximum current gain of only 128.

Keywords: 4H-SiC, lateral bipolar junction transistor (BJT), high current gain, high breakdown voltage

PACS: 72.80.Ey, 73.40.Kp, 73.40.Qv **DOI:** 10.1088/1674-1056/22/9/097201

1. Introduction

Power bipolar junction transistors (BJTs) based on 4H-SiC are recognized as very attractive candidates for usage in high-power switching devices. For the best use of the advantages of 4H-SiC BJTs, they can be used in high temperature environments because they are free of gate-oxide reliability issues as compared with the MOS transistors. In order to avoid significant power losses at the base-drive circuit, a high current gain is needed. Although several studies have been reported to increase the current gain by optimizing device geometry[1–3] surface passivation[4,5] or with double base epilayer[6] or base with buried layer[7] 4H-SiC BJT reported in the literature exhibits a very low current gain typically in a range of 60–70.[1,8] In recent years, a few groups have achieved current gains over 100[9–12] at room temperature. In addition, a group has achieved a high current gain exceeding 200 in 2011 by using state-of-the-art surface passivation combined with an intentional deep-level-reduction process based on thermal oxidation.[13] All the investigations above are based on vertical bipolar junction transistors (VBJTs). As is well known, apart from surface recombination, base width is an important limiting factor of current gain. Current gain can be increased dramatically by reducing the base width. However, if the base width is too low, a complete depletion of base region can happen before the initiation of impact ionization-induced breakdown at the base-collector junction, causing what is known as punch-through breakdown. Therefore, there is little room for optimizing base width to acquire a trade-off between high current gain and high breakdown voltage (V_{BR}) for a vertical BJT. Moreover, vertical structures are not easy to be integrated with other circuit components to develop power integrated circuits.

In this paper, we mainly focus on a 4H-SiC lateral BJT and a novel lateral BJT structure is proposed with surface electric field optimization technique including a field plate and a double reduced surface field (RESURF), which is used to achieve high breakdown voltage and lower specific on-resistance (R_{ON_SP}). More importantly, a base field plate can restrict collector-base depletion extension in the base region. Therefore, a high current gain with thin base as well as low base doping can be obtained under the condition of high avalanche breakdown.

The two-dimensional numerical analysis tool ATLAS[14] is used to investigate the electrical characteristics. An LBJT with high voltage above 3300 V is designed with little depletion in the base region. Influences of base width on current gain and breakdown voltage are studied, by which a maximum current gain of 247 with $V_{BR} = 3309$ V is achieved. Finally, vertical BJT with a comparable breakdown voltage of 3357 V is also analyzed. Simulation results indicate that the current gain of an LBJT is almost twice as high as that of an optimum VBJT under the comparable avalanche breakdown voltage.

2. Device structure and physical model

A schematic cross-sectional view of the proposed lateral 4H-SiC BJT is shown in Fig. 1. A traditional P-type RESURF epilayer is grown at the top of the P^+ substrate with an acceptor doping of 2×10^{15} cm^{-3}. The N-type epilayer with a

*Project supported by the Ministry of Education of China (Grant No. 20100101110056) and the Natural Science Foundation for Distinguished Young Scholars of Zhejiang Province of China (Grant No. R1100468).

†Corresponding author. E-mail: xielyz@zju.edu.cn

© 2013 Chinese Physical Society and IOP Publishing Ltd

thickness of 2 μm is doped with 4.5×10^{16} cm^{-3}. Region I in Fig. 1 is defined as the drift region and its length is 30 μm, targeting a breakdown voltage above 3300 V. As shown in the figure, an additional top RESURF region is added inside the N epilayer, making this a double RESURF structure. The top RESURF (16 μm long and 0.5 μm deep) is used to modulate the surface electric field distribution. Doping and width of the P-type base epilayer are varied in our investigation and will be discussed later in the paper. The emitter layer consists of a 0.3-μm nitrogen-doped epilayer to 5×10^{19} cm^{-3}. Besides, base field plate and collector field plate with oxide thickness (T_{OX}) of 0.5 μm are applied. The length of the collector field plate (L_{CFP}) is 6 μm. The parameter L_{BFP} refers to the base field plate length. The area of simulated device is set to be 1 cm^2 for simplicity of evaluation. A temperature of 300 K is employed as default in the simulations.

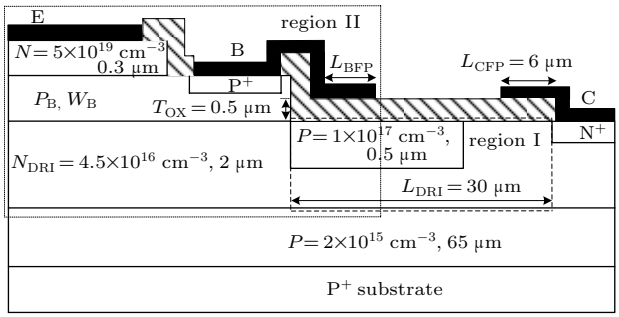


Fig. 1. Schematic structure of the lateral 4H-SiC BJT.

The most important models for 4H-SiC used in the simulations are given below.[15]

i) SRH recombination with carrier time of $\tau_n = 5\tau_p$ ($\tau_p = 10$ ns), including doping concentration and temperature dependence.[16]

ii) Auger recombination with Auger coefficients: electrons are of 5×10^{-29} cm^6/s and holes are defined as 9.9×10^{-32} cm^6/s.[17]

iii) Surface recombination: acceptor-like density state function to be modeled. A constant state density of traps D_{it} equals 2×10^{12} cm^{-2}·eV^{-1} and capture cross section 1×10^{-15} cm^2 with degeneracy factor of 1.0 are used.[16,18]

iv) Incomplete ionization for both n (nitrogen) doping and p (aluminum) doping. For nitrogen donor levels in 4H-SiC, a dopant ionization energy is 65 meV and $g_c = 2$. The p-type doping can be achieved with aluminum acceptors with an ionization energy of 191 meV and $g_v = 4$.[19]

v) Bandgap narrowing according to the model proposed by Lindefelt.[20]

3. Simulation results and discussion

Figure 2 shows the potential distribution in Region II and depletion in the base region when breakdown happens for two cases: with a double RESURF only in the drift region; with base field plate ($L_{BFP} = 8$ μm) and oxide ($T_{OX} = 0.5$ μm) as well as a double RESURF. The doping of the drift region (N_{DRI}) is kept to be 4.5×10^{16} cm^{-3} for both cases. Figure 3 shows the corresponding surface electric field distributions in the drift region (Region I).

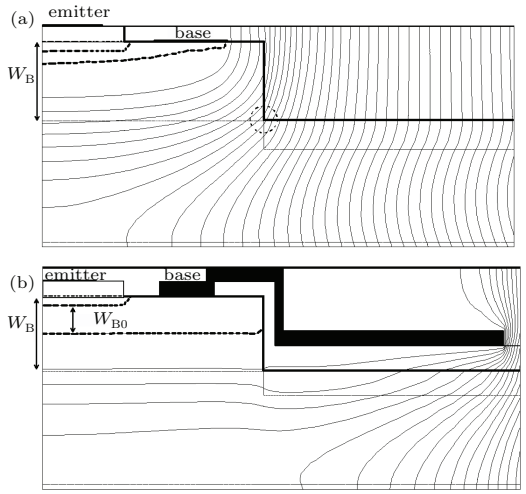


Fig. 2. Potential distribution in Region II and depletion extension in the base region when breakdown happens for two cases: (a) with a double RESURF only; (b) with base field plate ($L_{BFP} = 8$ μm) and oxide ($T_{OX} = 0.5$ μm) as well as a double RESURF. $L_{CFP} = 6$ μm. In both cases: $P_B = 1. \times 10^{17}$ cm^{-3}, $W_B = 1.5$ μm, and $L_{DRI} = 30$ μm.

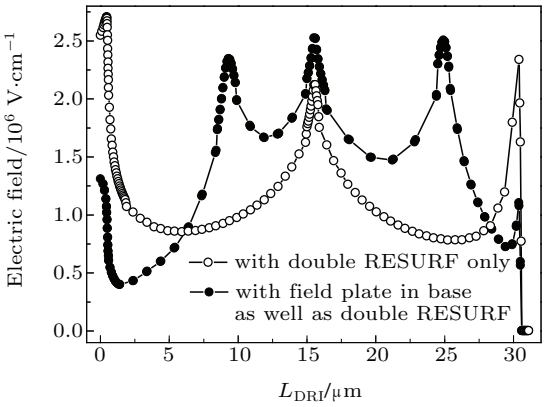


Fig. 3. Surface electric field distributions in Region I for the cases in Fig. 2.

As can be seen in Fig. 2(a) with drift region doping of 4.5×10^{16} cm^{-3}, collector-base depletion extends into the base region so much that base must be kept thick enough to guarantee that punch through does not happen under high bias. A thick base is an obstacle the needs to be overcome to acquire a high current gain for an LBJT. When the field plate is attached to the base, potential lines crowding at the place marked with dotted circle in Fig. 2(a) are pushed away. Electric field peak is reduced to a much lower level than that with a double RESURF only. As shown in Fig. 2(b), for the LBJT a base field plate, depletion extension into the base region becomes much smaller than that without field plate. This is pretty favorable to making a BJT with thin base and high current gain.

Figure 3 shows corresponding surface electric field distributions in the LBJT for the cases in Fig. 2. As seen clearly, the peak surface electric field moves far from the base region. This indicates that a thinner base can be used, which will lead to a higher current gain.

To achieve an LBJT with breakdown voltage over 3300 V, $L_{\rm DRI}$ is designed to be 30 μm. Collector field plate of 6 μm long ($L_{\rm CFP}$) is used to reduce electric field at the N/N$^+$ junction. Oxide thickness ($T_{\rm OX}$) is set to be 0.5 μm. Neutral base width is denoted as $W_{\rm B0}$ (see Fig. 2(b)). A wider neutral base means less collector-base junction depletion in the base region. Breakdown voltage and neutral base width ($W_{\rm B0}$) each as a function of the base field plate length ($L_{\rm BFP}$) are investigated to find the optimal $L_{\rm BFP}$ and the results are shown in Fig. 4.

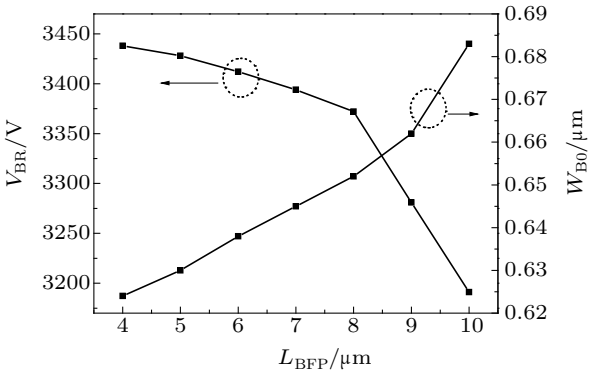


Fig. 4. Breakdown voltage ($V_{\rm BR}$) and neutral base width ($W_{\rm B0}$) versus base field plate length ($L_{\rm BFP}$). $L_{\rm CFP} = 6$ μm, $T_{\rm OX} = 0.5$ μm, $P_{\rm B} = 1 \times 10^{17}$ cm^{-3}, $W_{\rm B} = 1.5$ μm, and $L_{\rm DRI} = 30$ μm.

From this figure, it can be seen that when $L_{\rm BFP}$ increases from 4 μm to 10 μm, $V_{\rm BR}$ decreases while $W_{\rm B0}$ increases. It can be explained that electric field on the base side of the drift region (Region I) will be lowered with increasing $L_{\rm BFP}$ and the peak electric field moves to the end of the base field plate. As a consequence, breakdown voltage is reduced. However, due to the lowered electric field on the base side of drift region, collector-base depletion in the base region is suppressed and neutral base width can be kept high. From simulation results shown in Fig. 4, when $L_{\rm BFP}$ equals 8 μm, breakdown voltage decreases to 3376 V, and neutral base width increases to 0.65 μm. If $L_{\rm BFP}$ increases to exceed 8 μm, $V_{\rm BR}$ will become lower than 3300 V, which does not meet our design goal of breakdown voltage, i.e., greater than 3300 V. Therefore, $L_{\rm BFP} = 8$ μm is chosen to be an optimized value, and then the least depletion in the base region is obtained under breakdown voltage above 3300 V.

Based on an optimal base field plate length of 8 μm current gains and breakdown voltages each as a function of base width ($W_{\rm B}$) for different values of base doping ($P_{\rm B}$) in an LBJT are studied. The base width is varied from 0.3 μm to 1.5 μm. Simulation results are shown in Fig. 5(a).

As can be seen from Fig. 5(a), when $W_{\rm B}$ ranges from 0.4 μm to 1.5 μm, the breakdown voltage of designed lateral 4H-SiC BJT can be kept at a high level (3370 V) for base doping of 3×10^{17} cm^{-3}. When $W_{\rm B}$ is reduced to 0.32 μm, a current gain of 247 is obtained. At the same time the breakdown voltage is still kept above 3300 V (3309 V in Fig. 5(a)). When $P_{\rm B}$ is reduced to 2×10^{17} cm^{-3}, the maximum current gain we can obtain is only 72 when $V_{\rm BR}$ exceeds 3300 V. Lower base doping makes punch through happen more easily under high voltage. When base doping increases to 4×10^{17} cm^{-3}, the thinnest base with $V_{\rm BR}$ over 3300 V is 0.3 μm, and the corresponding current gain is 228. A higher base doping can indeed lead to a thinner base. However it will create more holes recombined with electrons in the base region. This will prevent the improvement in the current gain.

For comparison, conventional vertical BJT (VBJT) with a comparable breakdown voltage of 3300 V is also investigated using the ATLAS simulator under the same physical models mentioned above. The drift region length of 20 μm and doping of 3×10^{15} cm^{-3} are used. Current gains and breakdown voltages varying with the base width for different values of base doping are shown in Fig. 5(b). For the VBJT, the breakdown voltage drops more quickly than that of an LBJT as $W_{\rm B}$ decreases. When the base doping increases to 8×10^{17} cm^{-3}, the maximum current gain of 128 is obtained for $W_{\rm B} = 0.25$ μm.

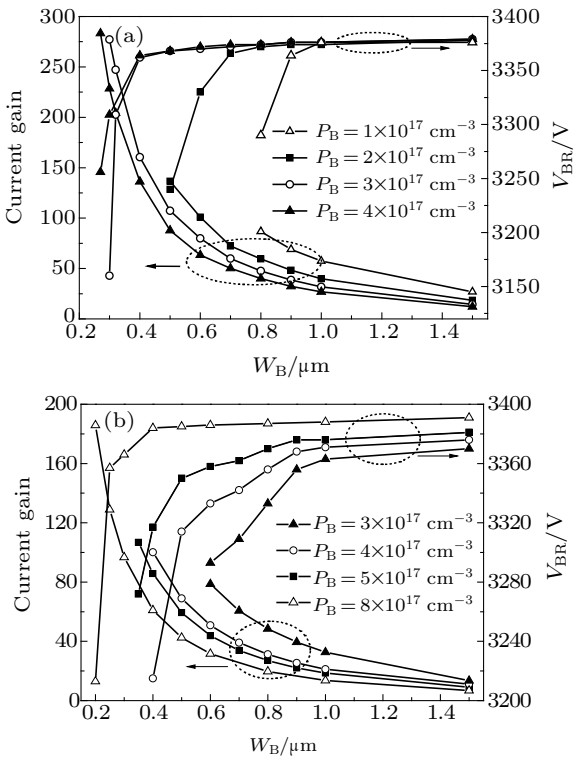


Fig. 5. Current gain and breakdown voltage each as a function of base width ($W_{\rm B}$) for different values of base doping ($P_{\rm B}$). (a) For the LBJT: $L_{\rm DIR} = 30$) μm and $N_{\rm DRI} = 4.5 \times 10^{16}$ cm^{-3}; (b) for the VBJT: $L_{\rm DIR} = 20$) μm and $N_{\rm DRI} = 3 \times 10^{15}$ cm^{-3}.

The maximum current gains with $V_{\rm BR}$ above 3300 V for each base doping ($P_{\rm B}$) ranging from 1×10^{17} cm^{-3} to 9×10^{17} cm^{-3} for the LBJT and the VBJT are shown in Fig. 6.

As can be seen from the figure, for an LBJT, when P_B increases from 1×10^{17} cm^{-3} to 3×10^{17} cm^{-3}, the maximum current gain with V_{BR} above 3300 V keeps increasing. The reason is that increasing P_B can cause a lower base width. Although increasing base doping will create more holes, a lower base width could significantly reduce carrier recombination in the base region. Therefore, the transportation factor of SiC BJT is improved and high current gain can be achieved. However, when the base doping increases to 4×10^{17} cm^{-3} or even higher, the reduced carrier recombination in the base region cannot compensate for the loss of current gain because of increased holes. Maximum current gain is therefore reduced. While for the VBJT, the maximum current gain of only 128 is achieved with a much higher base doping of 8×10^{17} cm^{-3}.

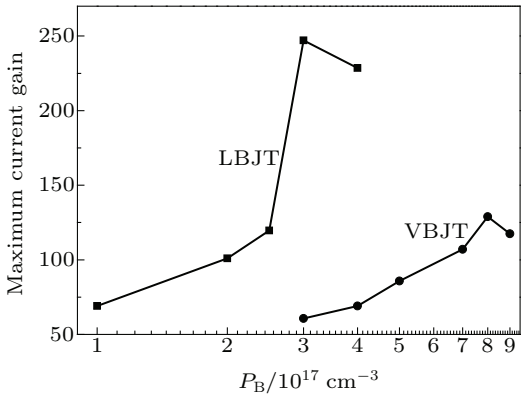


Fig. 6. Maximum current gains with breakdown voltage over 3300 V versus base doping (P_B). For the LBJT, L_{DIR} = 30 μm and $N_{DRI} = 4.5 \times 10^{16}$ cm^{-3}; for VBJT, L_{DIR} = 20 μm and $N_{DRI} = 3 \times 10^{15}$ cm^{-3}.

Table 1. Comparison of an optimal LBJT and VBJT with comparable V_{BR} of 3300 V.

	LBJT	VBJT
V_{BR}/V	3309	3357
Current gain	247	128
R_{ON_SP}/mΩ·cm^2	22.9	8.16

DC *I–V* output characteristics of the LBJT and the VBJT are shown in Fig. 6 with base current (I_B) ranging from 200 mA to 1000 mA. Breakdown voltage, current gain, and specific on-resistance of an optimum LBJT and VBJT are listed in Table 1. From Fig. 6, it can be seen that when the optimum LBJT device conducts a collector current of 100 A/cm^2, and the forward voltage drop is 2.29 V, which corresponds to a specific on-resistance of 22.9 mΩ·cm^2. Although a double RESURF structure is applied, the designed LBJT still presents a specific on-resistance higher than that of the VBJT, whose specific on-resistance R_{ON_SP} is only 8.16 mΩ·cm^2 (collector voltage of 0.816 V and collector current of 100 A/cm^2). Because the required drift region is added to the lateral dimension of the device, the lateral BJT tends to require a large SiC chip area compared with the vertical BJT for the same on-resistance. The areas of simulated devices including the LBJT and the VBJT in this paper are all set to be 1 cm^2, which is considered to be the reason for the higher specific on-resistance of the LBJT. Application of a double RESURF leads to a narrower current channel in the drift region under P top region, which also contributes to a higher R_{ON_SP}. For such a general disadvantage of lateral power devices, it is believed that by improving the structure, the specific on-resistance of the LBJT will be optimized to an acceptable value.

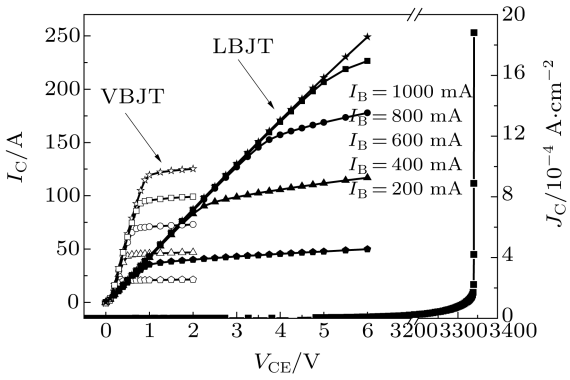


Fig. 7. DC *I–V* output characteristics of the 4H-SiC LBJT and VBJT. Both the LBJT and the VBJT are optimized with maximum current gain under V_{BR} above 3300 V. For the LBJT, $P_B = 3 \times 10^{17}$ cm^{-3} and $W_B = 0.32$ μm; for VBJT, $P_B = 8 \times 10^{17}$ cm^{-3} and $W_B = 0.25$ μm. The area of simulated devices is set to be 1 cm^2.

4. Conclusions

In this paper, a lateral 4H-SiC BJT is investigated and a new structure with a double RESURF and a base field plate is presented. Compared with the LBJT with a double RESURF only, combining a base field plate and double RESURF is proved to be effective in reducing depletion in the base region. Simulation results indicate that when the base field plate length is 8 μm, the least depletion in the base region can be obtained. At the same time, the breakdown voltage higher than 3300 V can be achieved at $L_{DRI} = 30$ μm. Then, influences of the base width on current gain and breakdown for different values of base doping are investigated in an LBJT with $L_{BFP} = 8$ μm. When the base width is reduced to 0.32 μm with a base doping of 3×10^{17} cm^{-3}, the maximum current gain of 247 with high voltage of 3309 V is achieved. For comparision, influences of the base width in VBJT are studied with comparable V_{BR} up to 3300 V. For VBJT, a maximum current gain of 128 is obtained with $W_B = 0.25$ μm and $P_B = 8 \times 10^{17}$ cm^{-3}. The optimum LBJT shows an overwhelming advantage over the VBJT on current gain, of which the ratio is 247, much higher than 128. Nevertheless, the optimum LBJT has a specific on-resistance of 22.9 mΩ·cm^2, which is significantly higher than that of VBJT (only 8.16 mΩ·cm^2). It is concluded that the proposed LBJT can be an excellent candidate for high-current gain and high breakdown, especially in power integrated circuits.

References

[1] Domeij M, Lee H S, Danielsson E, Zetterling C M, Ostling M and Schoner A 2005 *Electron Dev. Lett.* **26** 743

[2] Yan G, Huang A Q, Krishnaswami S, Agarwal A K and Scozzie C 2006 5*th International Power Electronics and Motion Control Conference* August 14-16 2006 Shanghai, China p. 1

[3] Buono B, Ghandi R, Domeij M, Malm B G, Zetterling C M and Ostling M 2010 *Electron Dev.* **57** 2664

[4] Ghandi R, Buono B, Domeij M, Esteve R, Schoner A and Han J S 2011 *Electron Dev.* **58** 259

[5] Miyake H, Kimoto T and Suda J 2011 *Electron Dev. Lett.* **32** 285

[6] Zhang Q, Zhang Y M, Yuan L, Zhang Y M, Tang X Y and Song Q W 2012 *Chin. Phys. B* **21** 088502

[7] Zhang Y R, Zhang B, Li Z J, Deng X C and Liu X L 2009 *Chin. Phys. B* **18** 3995

[8] Zhang J H, Li X Q, Alexandrov P, Fursin L, Wang X H and Zhao J H 2008 *Electron Dev.* **55** 1899

[9] Zhang Q, Agarwal A, Burk A, Geil B and Scozzie C 2008 *Solid State Electron.* **52** 1008

[10] Nonaka K, Horiuchi A, Negoro Y, Iwanaga K, Yokoyama S, Hashimoto H, Sato M, Maeyama Y, Shimizu M and Iwakuro H 2009 *Mater. Sci. Forum* **615** 821

[11] Miyake H, Kimoto T and Suda J 2011 *Electron Dev. Lett.* **32** 285

[12] Domeij M, Konstantiov A, Lindgren A, Zaring C, Gumaelius K and Reimark M 2012 *Mater. Sci. Forum.* **717** 1123

[13] Miyake H, Kimoto T and Suda J 2011 *Electron Dev. Lett.* **32** 841

[14] Device Simulator Atlas 2008 *Atlas User's Manual* (Silvaco International)

[15] Ruff M, Mitlehner H and Helbig R 1994 *Electron Dev.* **41** 1040

[16] Kordina O, Bergman J, Hallin C and Janzen E 1996 *Appl. Phys. Lett.* 69

[17] Galeckas A, Linnros J, Grivickas V, Lindefelt U and Hallin C 1997 *Appl. Phys. Lett.* **71** 3269

[18] Zhang Y R, Zhang B, Li Z J and Deng X C 2010 *Chin. Phys. B* **19** 067102

[19] Troffer T, Schadt M, Frank T, Itoh H, Pensl G, Heindl J, Strunk H and Marier M 1997 *Phys. Stat. Sol.* **162** 277

[20] Lindefelt U 1998 *J. Appl. Phys.* **84** 2628